

# SOLID STATE CONFORMATIONAL FLEXIBILITY AT WORK: ZIPPING AND UNZIPPING A CYCLIC PEPTOID SINGLE CRYSTAL

Alessandra Meli,<sup>[a]</sup> Eleonora Macedi,<sup>[a]</sup> Francesco De Riccardis,<sup>[a]</sup> Vincent J. Smith,<sup>[b]</sup> Leonard J. Barbour,<sup>[b]</sup> Irene Izzo,<sup>\*[a]</sup> Consiglia Tedesco<sup>\*[a]</sup>

---

Dr. A. Meli, Dr. E. Macedi, Prof. F. De Riccardis, Prof. I. Izzo, Dr. C. Tedesco  
Dipartimento di Chimica e Biologia "A. Zambelli"  
Università degli Studi di Salerno,  
Via Giovanni Paolo II 132, I-84084 Fisciano (SA), Italy  
E-mail: ctedesco@unisa.it; iizzo@unisa.it

[b] Dr. V. J. Smith, Prof. L. J. Barbour  
Department of Chemistry and Polymer Science,  
University of Stellenbosch,  
Private Bag X1, 7602 Matieland, Stellenbosch, South Africa.

**Abstract:** A peptidomimetic compound undergoes a reversible single-crystal to single-crystal transformation upon guest release/uptake involving a drastic conformational change of the macrocycle. The pervasive movement (more than 110°) of two side chains is triggered by the disruption of CH- $\pi$  host-guest interactions and is followed by the formation of new CH- $\pi$  interactions between the moving side chains. The extensive and reversible alteration in the solid state is connected to the formation of an unprecedented "CH- $\pi$  zipper", which reversibly opens and closes, thus allowing for guest sensing.

The biological processes of living systems rely on control of the dynamic behavior of biomolecules.<sup>[1]</sup> The intrinsic flexibility of proteins enables accurate guest recognition and specific substrate conversion.<sup>[2]</sup> Most of the polypeptides' functions are accomplished in fluids (water or non-polar phases) and constitute the essence of life. Enzymatic activity can also be tracked in protein crystals due to the presence of water channels that allow guest diffusion and dynamic fluctuation of active sites, while preserving crystal integrity and promoting catalysis.<sup>[3]</sup>

The design and synthesis of artificial systems able to mimic biological functions is the aim of inexhaustible research activity in the field of molecular nanotechnology.<sup>[4]</sup> In particular, one of the goals of crystal engineering is the quest for crystalline materials that combine the recognition abilities of protein crystals with thermochemical stability.<sup>[4b]</sup>

Guest-induced single-crystal to single-crystal (SCSC) transformations have mainly been observed in metal-organic frameworks or coordination polymers.<sup>[5]</sup> In these cases the strength and directionality of the metal coordination bonds provide a robust architecture preserving the crystals from disruption in spite of large movements of the ligands.<sup>[6]</sup> Examples of guest-induced SCSC transformations are also reported for molecular compounds.<sup>[7]</sup> In the cases investigated the observed dynamic behavior consists of positional or orientational rearrangements of the molecules inside the crystals. Banerjee and coworkers<sup>[8]</sup> described a reversible SCSC transformation by solvent exchange in a peptide macrocycle. The removal of CHCl<sub>3</sub> at 165 °C alters the columnar arrangement of macrocycles from staggered to eclipsed. In a more recent example involving a peptoid molecule (octapeptoid), Kirshenbaum *et al.*<sup>[10]</sup> report only a negligible rearrangement of the host molecule during water uptake and release. .

*This is the pre-peer reviewed version of the following article: A. Meli, E. Macedi, F. De Riccardis, V. J. Smith, L. J. Barbour, I. Izzo, C. Tedesco, Angew Chem Int Ed Eng. 2016 Apr 4; 55(15):4679-82, which has been published in final form at doi: [10.1002/anie.201511053](https://doi.org/10.1002/anie.201511053). This article may be used for non-commercial purposes in accordance with Wiley Terms and Conditions for Use of Self-Archived Versions.*

Herein we report the first example of a reversible SCSC transformation induced by guest removal and which, most notably, involves a drastic *conformational* change of the host. The molecular host compound **1** (Figure 1), decorated by strategically arrayed propargyl/methoxyethyl side chains, belongs to the family of the cyclic peptoids. The disruption of CH- $\pi$  host-guest interactions<sup>[9]</sup> induces a conspicuous movement (more than 110°) of two propargyl side chains, generating new stabilizing CH- $\pi$  interactions and forming an unprecedented reversible “CH- $\pi$  zipper”.

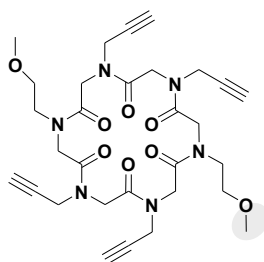


**Figure 1.** Cyclo-(*Nme-Npa*)<sub>2</sub> **1**. *Nme* = *N*-(methoxyethyl)glycine, *Npa* = *N*-(propargyl)glycine.

Peptoids differ from peptides in the position of the side chains in the backbone: in peptides they are linked to the stereogenic carbon atoms while in peptoids they are attached to the nitrogen atoms (giving *N*-substituted oligoglycines, Figure 2a).<sup>[11]</sup> The lack of the amide protons prevents the formation of NH $\cdots$ OC hydrogen bonds and weaker interactions, such as CH $\cdots$ OC hydrogen bonds.<sup>[12]</sup> Moreover, CH- $\pi$  interactions<sup>[13]</sup> now play a key role in the formation of secondary structures.<sup>[14]</sup>

In comparison to the corresponding peptides, the presence of tertiary amide bonds adds further flexibility to the peptoid backbone: the *cis/trans* conformations are, in fact, almost isoenergetic (Figure 2b).<sup>[14]</sup>

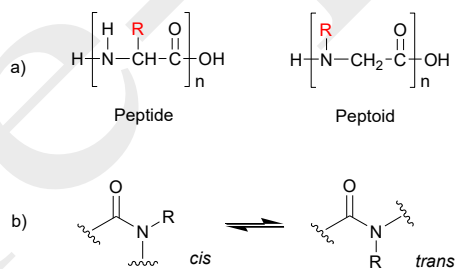


**Figure 2.** a) A comparison of the peptide and peptoid structures; b) *cis/trans* conformational isomerism in tertiary amides.

A useful strategy to increase the conformational rigidity of linear oligomers is achieved through head-to-tail cyclization.<sup>[15]</sup> In particular, it has been demonstrated that cyclic peptoids may even encode reverse-turn type secondary structures.<sup>[15k]</sup>

In a recent survey of the solid state assembly of free and metal coordinated cyclic  $\alpha$ -peptoids<sup>[16]</sup> we concluded that: 1) the columnar arrangement of macrocycles is stabilized by interannular face to face or side by side CH $\cdots$ OC hydrogen bonds (mimicking the  $\beta$ -sheet secondary structure in peptides) and 2) side chains have a major impact on the solid-state assembly of cyclic  $\alpha$ -peptoids. For example methoxyethyl and propargyl side chains serve as pillars, inducing a columnar arrangement of the peptoid macrocycles.<sup>[15d, 16]</sup>

These observations prompted us to design and synthesize compound **1** (Figure 1), displaying two distal methoxyethyl side chains and four propargyl side chains. Our goal was to verify the columnar arrangement of the macrocycles and to study possible host/guest properties as a prelude to their application in molecular storage, separation and catalysis.

The linear precursor of *cyclo-(Nme-Npa)<sub>2</sub>* **1** (Scheme S1, Supporting Information) was prepared using the efficient sub-monomer approach introduced by Zuckerman *et al.*<sup>[17]</sup> In a two-step sequence, repeated iteratively, each monomer is constructed on the 2-chlorotrityl resin from the C- to the N-terminus using *N,N'*-diisopropylcarbodiimide-mediated acylation with bromoacetic acid, followed by amination with the commercially available propargyl amine or methoxyethyl amine. The hexameric oligomer was cleaved from the resin and cyclized under high dilution conditions ( $3.0 \times 10^{-3}$  M) in the presence of the efficient coupling agent HATU.<sup>[15i,k]</sup>

Compound **1** was crystallized from hot acetonitrile. The X-ray crystal structure corresponds to an acetonitrile solvate (form **1A**) with a 1:2 ratio between cyclopeptoid and acetonitrile molecules (the unit cell contains two cyclopeptoid and four acetonitrile molecules).<sup>[18]</sup> The macrocycle possesses a crystallographic inversion centre. It exhibits a *cctcct* sequence of distorted amide bonds, two methoxyethyl and two propargyl side chains pointing vertically up and down with respect to the macrocycle plane, and two propargyl side chains extending horizontally in the equatorial directions.

As shown in Figure 3a (top), the molecules align in a columnar arrangement along the shortest *c* axis through CO $\cdots$ HC interactions involving the carbonyl groups of the peptoid backbone and the terminal hydrogen atom of the vertical propargyl side chain (CO $\cdots$ HC 2.20 Å, O $\cdots$ HC angle 163°). Differently from analogous compounds,<sup>[15d]</sup> the methoxyethyl side chains are not involved in the CO $\cdots$ HC interactions. The horizontal propargyl side chains interact with the vertical propargyl side chains of the proximal cyclopeptoid molecules *via* CH- $\pi$  interactions (involving the methylene atoms as H donors and the triple bond  $\pi$  system). As shown in Figure 3b (top, and figure S3 in the Supporting Information), the acetonitrile molecules occupy the void space between the cyclopeptoid columns, which consists of channels parallel to the *c* axis (7 Å and 5 Å are maximum and minimum diameters, respectively). Acetonitrile molecules are linked together by means of CH- $\pi$  interactions (N $\equiv$ C $\cdots$ HC 2.81 Å) and are only weakly bound by means of the methyl hydrogen atoms to one carbonyl oxygen atom (CO $\cdots$ HC 2.48 Å) and to the equatorial propargyl triple bond (C $\equiv$ C $\cdots$ HC 2.87 Å).

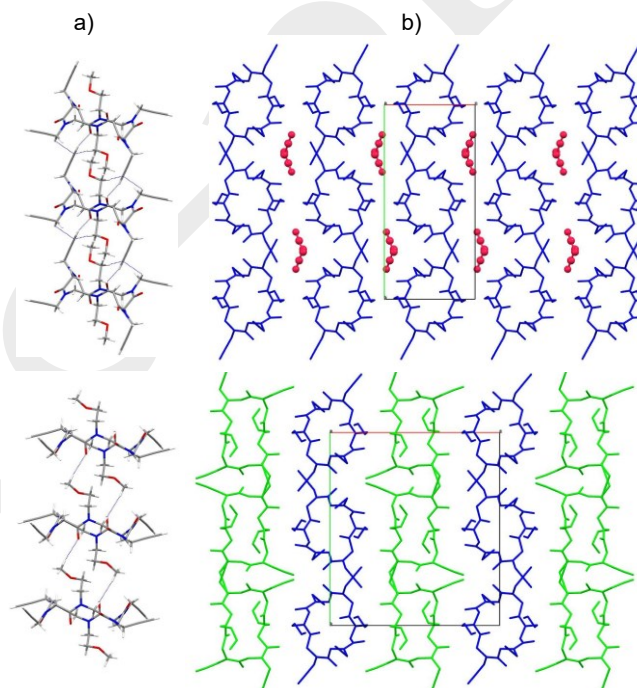


**Figure 3.** a) Columnar arrangement of cyclopeptoid molecules along the *c* axis in forms **1A** (top) and **1B** (type II molecules, bottom). CH- $\pi$  and CH $\cdots$ OC hydrogen bonds are depicted as blue dotted lines (atom type: C gray, H white, N blue, O red); b) crystal packing as viewed along the *c* axis in forms **1A** (top) and **1B** (bottom). Acetonitrile molecules in form **1A** (top) are shown in red. Form **1B** contains two crystallographically independent molecules, respectively blue and green. The blue ones show only slight differences with respect to form **1A**, while the green molecules are profoundly different.

Differential scanning calorimetry (DSC) analysis of crystals of form **1A** showed that acetonitrile molecules are released in the range 30-85°C. Melting occurs at 225 °C, followed by decomposition of the cyclic peptoid (Figure S4 in the Supporting Information). Thermogravimetric analysis (TGA) confirms the release of acetonitrile molecules between 30 °C and 65 °C (Figure S5 in the

Supporting Information). The observed percentage weight loss (~12%) is consistent with the loss of two acetonitrile molecules per cyclopeptoid molecule.

Hot stage microscopy (HSM) demonstrated that guest release (in the range 30-70°C) does not affect the shape of the crystals but only their transparency (Figure 4 and Movie 1 in the Supporting Information). After thermal treatment on the hot stage microscope a single crystal was selected and analyzed by single-crystal X-ray diffraction. The structure determination confirmed that all of the acetonitrile molecules were removed to give the desolvated form **1B** with no loss of crystal singularity (Figure S2 in Supporting information).<sup>[18]</sup>

In the desolvated form **1B** half of the cyclopeptoid molecules adopt a completely different conformation, in order to efficiently occupy the space left by the acetonitrile molecules (Figure 3b, bottom).<sup>[19]</sup>

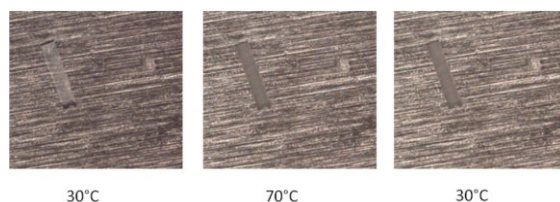


Figure 4. Hot stage microscopy: a single crystal of **1A** during thermal treatment from 30 °C to 70 °C and back to 30 °C.

Indeed, the crystals of **1B** contain two crystallographically independent cyclopeptoid molecules (blue and green, as reported in Figure 3b). Both are located around a crystallographic inversion center. The blue molecules (type I) show only slight differences with respect to form **1A**, while the green molecules (type II) register a dramatic change.

In type II (Figure 3a bottom) the two vertical propargyl side chains have moved horizontally with respect to the plane of the macrocycle. The propargyl torsion angle  $\chi_1$  changes from  $-118^\circ$  (in form **1A**) to  $129^\circ$  in type II, with an overall variation of  $113^\circ$ . Type II molecules stack on top of each other with the methoxyethyl side chains ( $\text{CH}_3 \cdots \text{O} \ 2.57 \text{ \AA}$ ,  $\text{O} \cdots \text{H-C} \ 171.4^\circ$ ) located between the macrocyclic rings, as clearly shown in Figure 3a (bottom).

The dramatic change in the orientation of the side chain is also accompanied by a peptoid backbone conformational adjustment: type II molecules (green) have a rather elongated rectangular shape with respect to the more circular type I molecules (blue). The observed rectangular shape is as a consequence of the ability of the peptoid backbone to adapt to an ideal type I  $\beta$ -turn structure.<sup>[20]</sup>

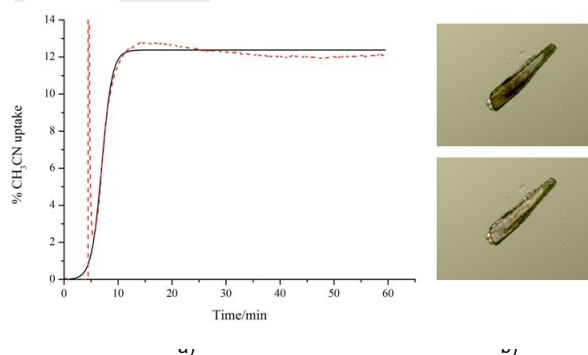


Figure 5. a) Sorption balance analysis on single crystals of **1B**. Red dashed line: experimental curve (the initial spike is due to the solvent injection); black solid line: sigmoidal curve-fitting; b) Optical microscope polarized light micrographs of a crystal of form **1B** before (top) and after (bottom) exposure to acetonitrile vapors.

The loss of acetonitrile molecules is accompanied by shrinkage of the crystal and a decrease in the unit cell volume of 11.6% (see Supporting Information).

Desolvated crystals are able to absorb the acetonitrile molecules, as demonstrated by soaking a desolvated crystal in acetonitrile for a few seconds and analyzing it by single-crystal X-ray diffraction at 100 K (Table S1, Supporting Information). The

reversibility was also verified by exposing crystals of form **1B** to acetonitrile vapors at 25 °C on an automated suspension microbalance<sup>[21]</sup> and measuring the weight increase during solvent uptake (Figure 5a). The weight percentage increase owing to the absorption of acetonitrile vapor is 11.8%, which agrees well with the stoichiometry of the crystal form **1A**.

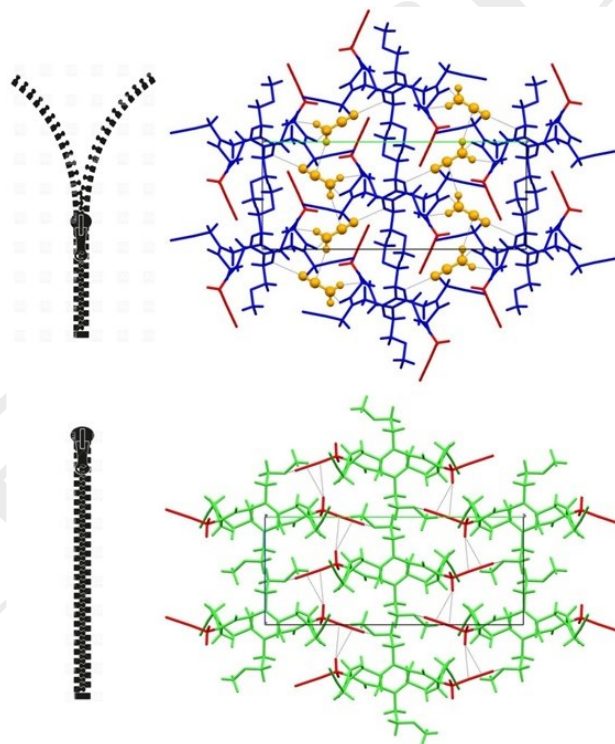
Moreover, by using optical microscopy with polarized light, a desolvated single crystal was observed while exposed to acetonitrile vapors. The acetonitrile uptake can be clearly detected in the recorded images (Figure 5b and Movie 2) showing the change in the aspect of the crystal with time.

These results suggest that the dynamic behavior of the cyclopeptoid molecules in the crystal may be described as correlated motion, where all movements of both cyclopeptoid and acetonitrile molecules are synchronized.<sup>[7c, 22]</sup>

As the acetonitrile molecules are released, the corresponding void volumes are occupied by propargyl side chains that move to the equatorial plane and provide intercolumnar CH- $\pi$  interactions between methylene H atoms and propargyl triple bonds of adjacent columns ( $C\equiv C\cdots HC$  2.80 Å,  $C\cdots H-C$  164.4°), acting as a "CH- $\pi$  zipper" (Figure 6).

The crystals release the guest molecules and close the CH- $\pi$  zipper by rotating the vertical propargyl side chains by more than 110°. They are then also able to sense the guest molecules and respond by opening the CH- $\pi$  zipper by moving the propargyl side chain back again in a synchronized fashion, thus allowing for guest uptake.

**Figure 6.** Open CH- $\pi$  zipper in the crystal form **1A** (top) and closed CH- $\pi$  zipper in the crystal form **1B** (bottom). Inter-columnar CH- $\pi$  interactions in form **1B** involve methylene H atoms and the propargyl triple bond of adjacent columns, replacing the released acetonitrile molecules (in yellow). Moving propargyl side chains are depicted in red, CH- $\pi$  bonds as grey dotted lines.



This work illustrates how conformational flexibility in organic macrocycles may be exploited to lead to functional materials, featuring both robustness and adaptivity. In particular, the suitable choice of the side chains has a key role in determining the solid state dynamic behavior of cyclic peptoids.

Moreover, these results suggest that easily tunable cyclic peptoids may represent very promising building blocks at the frontier between material science and biology and may be capable of reversible guest recognition and sequestration.

## Acknowledgements

The research leading to these results has received funding from the People Programme (Marie Curie Actions) of the European Union's Seventh Framework Programme FP7/2007-2013/ under REA grant agreement n°PIRSES-GA-2012-319011. Financial support also from the University of Salerno (FARB).

**Keywords:** peptoids • single crystal to single crystal transformation • CH- $\pi$  interactions • conformational change

- [1] a) J. M. Berg, J. L. Tymoczko, L. Stryer, *Biochemistry*, 7th ed., W. H. Freeman, New York, **2012**; b) A. Fersht, *Structure and mechanism in protein science: a guide to enzyme catalysis and protein folding*, Macmillan, New York, **1999**.
- [2] K. Henzler-Wildman, D. Kern *Nature* **2007**, *450*, 964–972.
- [3] D. Bourgeois, A. Royant, *Curr. Opin. Struct. Biol.* **2005**, 538–547.
- [4] a) S. Erbas-Cakmak, D. A. Leigh, C. T. McTernan, A. L. Nussbaumer, *Chem. Rev.* **2015**, *115*, 10081–10206; b) D. Braga, F. Grepioni, *Making Crystals by Design*, Wiley-VCH, Weinheim, 2007; c) W. R. Browne, B. L. Feringa, *Nature Nanotech.* **2006**, *1*, 25–35.
- [5] a) S. Bureekaew, H. Sato, R. Matsuda, Y. Kubota, R. Hirose, J. Kim, K. Kato, M. Takata, S. Kitagawa, *Angew. Chem. Int. Ed.* **2010**, *49*, 7660–7664; b) T. K. Maji, R. Matsuda, S. Kitagawa, *Nat. Mater.* **2007**, *6*, 142–148.
- [6] J. Seo, R. Matsuda, H. Sakamoto, C. Bonneau, S. Kitagawa, *J. Am. Chem. Soc.* **2009**, *131*, 12792–12800.
- [7] a) M. A. Little, M. E. Briggs, J. T. A. Jones, M. Schmidtman, T. Hasell, S. Y. Chong, K. E. Jelfs, L. Chen, A. I. Cooper, *Nature Chem.* **2015**, *7*, 153–159; b) J. L. Atwood, L. J. Barbour, A. Jerga, *Angew. Chem. Int. Ed.* **2004**, *43*, 2948–2950; c) J. L. Atwood, L. J. Barbour, A. Jerga, B. L. Schottel, *Science* **2002**, *298*, 1000–1002.
- [8] S. Guha, M. G. B. Drew, A. Banerjee, *CrystEngComm* **2009**, *11*, 756–762.
- [9] M. Nishio, M., Hirota, Y. Umezawa, *The CH/ $\pi$  Interaction. Evidence, Nature, and Consequences*, Wiley-VCH, Weinheim, **1998**.
- [10] S. B. L. Vollrath, C. Hu, S. Bräse, K. Kirshenbaum, *Chem. Commun.* **2013**, *49*, 2317–2319.
- [11] a) J. Sun, R. N. Zuckermann, *ACS Nano* **2013**, *7*, 4715–4732; b) R. N. Zuckermann, *Pept. Sci.*, **2011**, *96*, 545–555; c) J. Seo, B.-C. Lee, R. N. Zuckermann in *Comprehensive Biomaterials, Vol. 2* (Ed. P. Ducheyne), Elsevier, **2011**, pp. 53–76; d) S. A. Fowler, H. E. Blackwell, *Org. Biomol. Chem.* **2009**, *7*, 1508 – 1524.
- [12] a) G. R. Desiraju, *Acc. Chem. Res.* **1991**, *24*, 290–296; b) G. R. Desiraju, T. Steiner, *The Weak Hydrogen Bond in Structural Chemistry and Biology*, Oxford Science Publication, Oxford, 1999.
- [13] a) M. Nishio, Y. Umezawa, J. Fantini, M. S. Weiss, P. Chakrabartie *Phys. Chem. Chem. Phys.*, **2014**, *16*, 12648–12683; b) M. Nishio, Y. Umezawa, K. Honda, S. Tsuboyama, H. Suezawa, *CrystEngComm*, **2009**, *11*, 1757–1788; c) M. Nishio, *CrystEngComm*, **2004**, *6*, 130–158.
- [14] a) J. A. Crapster, I. A. Guzei, H. E. Blackwell *Angew. Chem. Int. Ed.* **2013**, *52*, 5079–5084; b) J. R. Stringer, J. A. Crapster, I. A. Guzei, H. E. Blackwell, *J. Am. Chem. Soc.* **2011**, *133*, 15559–15567; c) B. Yoo, K. Kirshenbaum, *Curr. Opin. Chem. Biol.* **2008**, *12*, 714–721; d) C. W. Wu, K. Kirshenbaum, T. J. Sanborn, J. A. Patch, K. Huang, K. A. Dill, R. N. Zuckermann, A. E. Barron, *J. Am. Chem. Soc.* **2003**, *125*, 13525–13530.
- [15] a) M. L. Lepage, A. Meli, A. Bodlenner, C. Tarnus, F. De Riccardis, I. Izzo, P. Compain *Beilstein J. Org. Chem.* **2014**, *10*, 1406–1412; b) F. De Riccardis, C. De Cola, G. Fiorillo, A. Meli, S. Aime, E. Gianolio, I. Izzo, *Org. Biomol. Chem.*, **2014**, *12*, 424–431; c) G. Della Sala, B. Nardone, F. De Riccardis, I. Izzo, *Org. Biomol. Chem.*, **2013**, *11*, 726–731; d) I. Izzo, G. Ianniello, C. De Cola, B. Nardone, L. Erra, G. Vaughan, C. Tedesco, F. De Riccardis, *Org. Lett.* **2013**, *15*, 598–601; e) M. L. Huang, M. A. Benson, S. B. Y. Shin, V. J. Torres, K. Kirshenbaum *Eur. J. Org. Chem.* **2013**, 3560–3566; f) B. Yoo, S. B. Y. Shin, M. L. Huang, K. Kirshenbaum, *Chem. Eur. J.*, **2010**, *16*, 5528–5537; g) R. N. Zuckermann, T. Kodadek, *Curr. Opin. Mol. Ther.* **2009**, *11*, 299–307; h) C. De Cola, S. Lichen, D. Comegna, E. Cafaro, G. Bifulco, I. Izzo, P. Tecilla, F. De Riccardis, *Org. Biomol. Chem.* **2009**, *7*, 2851–2854; i) N. Maulucci, I. Izzo, G. Bifulco, A. Aliberti, C. De Cola, D. Comegna, C. Gaeta, A. Napolitano, C. Pizza, C. Tedesco, D. Flot, F. De Riccardis, *Chem. Commun.*, **2008**, 3927–3929; j) O. Roy, S. Faure, V. Thery, C. Didierjean, C. Taillefumier, *Org. Lett.* **2008**, *10*, 921–924; k) S. B. Y. Shin, B. Yoo, L. J. Todaro, K. Kirshenbaum, *J. Am. Chem. Soc.* **2007**, *129*, 3218–3225.
- [16] C. Tedesco, L. Erra, I. Izzo, F. De Riccardis *CrystEngComm* **2014**, *16*, 3667–3687.
- [17] R. N. Zuckermann, J. M. Kerr, S. B. H. Kent, W. H. Moos, *J. Am. Chem. Soc.* **1992**, *114*, 10646–10647.
- [18] Diffraction data for both crystal **1A** and **1B** forms were collected at 100 K with a Bruker Smart diffractometer equipped with an APEXII CCD detector using Mo  $K\alpha$  radiation.  
 Form **1A**: Formula  $C_{30}H_{38}N_6O_8 \cdot 2 CH_3CN$ , formula weight 692.77, monoclinic,  $P2_1/c$ ,  $a = 9.773(5) \text{ \AA}$ ,  $b = 20.961(10) \text{ \AA}$ ,  $c = 8.500(4) \text{ \AA}$ ,  $90.990(7)^\circ$ ,  $V = 1740.9(14) \text{ \AA}^3$ ,  $Z=2$ ,  $D_x = 1.322 \text{ g cm}^{-3}$ ,  $\mu = 0.096 \text{ mm}^{-1}$ ,  $R1 (I > 2\sigma) = 0.0465 (2960)$ ,  $wR2 (all) = 0.1173 (3594)$ ,  $\rho_{min} = -0.26 \text{ e \AA}^{-3}$ ,  $\rho_{max} = 0.28 \text{ e \AA}^{-3}$ .  
 Form **1B**: Formula  $C_{30}H_{38}N_6O_8$ , formula weight 610.66, monoclinic,  $P2_1/c$ ,  $a = 17.887(3) \text{ \AA}$ ,  $b = 20.335(3) \text{ \AA}$ ,  $c = 8.4716(12) \text{ \AA}$ ,  $93.160(2)^\circ$ ,  $V = 3076.7(8) \text{ \AA}^3$ ,  $Z=4$ ,  $D_x = 1.318 \text{ g cm}^{-3}$ ,  $\mu = 0.097 \text{ mm}^{-1}$ ,  $R1 (I > 2\sigma) = 0.0495 (5009)$ ,  $wR2 (all) = 0.1148 (7960)$ ,  $\rho_{min} = -0.26 \text{ e \AA}^{-3}$ ,  $\rho_{max} = 0.28 \text{ e \AA}^{-3}$ .  
 CCDC 1431223 (**1A** form) and CCDC 1431224 (**1B** form) contain the supplementary crystallographic data for this paper. These data are provided free of charge by The Cambridge Crystallographic Data Centre.
- [19] The values of the torsion angles in the macrocycles before and after the acetonitrile removal are reported in Table S2 of the Supporting Information.
- [20] It is worth noting that **1B** form type II molecules display the lowest rmsd value (0.142 Å) by superposition with type I  $\beta$ -turn idealized peptide structure, while Kirshenbaum reported a rmsd value of 0.397 Å for a similar cyclic peptoid<sup>[15k]</sup> (see Table S3 and Figure S6 in the Supporting Information).
- [21] L. J. Barbour, K. Achleitner, J. R. Greene, *Thermochim. Acta* **1992**, *205*, 171–177.
- [22] a) R. Katoono, H. Kawai, M. Ohkita, K. Fujiwara, T. Suzuki, *Chem. Commun.* **2013**, *49*, 10352–10354; b) K. Mislow, *Acc. Chem. Res.* **1976**, *9*, 26–33.